

Model for the transformation of an icosahedral phase into a B2 crystalline phase

This article has been downloaded from IOPscience. Please scroll down to see the full text article.

2008 J. Phys.: Condens. Matter 20 235215

(<http://iopscience.iop.org/0953-8984/20/23/235215>)

View [the table of contents for this issue](#), or go to the [journal homepage](#) for more

Download details:

IP Address: 129.252.86.83

The article was downloaded on 29/05/2010 at 12:32

Please note that [terms and conditions apply](#).

Model for the transformation of an icosahedral phase into a B2 crystalline phase

V S Kraposhin^{1,4}, A L Talis², Ha Thanh Lam¹ and J-M Dubois³

¹ Material Science Chair, Bauman Moscow State Technical University, 5, 2nd Baumanskaya Street, Moscow 105005, Russia

² A N Nesmeyanov Institute of Organoelement Compounds, Russian Academy of Science, 28, Vavilov Street, Moscow 119991, Russia

³ Laboratoire de Science et Génie des Matériaux et de Métallurgie, Ecole des Mines, Parc de Saurupt, 54042 Nancy Cedex, France

E-mail: kraposhin@mtu-net.ru

Received 17 March 2008

Published 6 May 2008

Online at stacks.iop.org/JPhysCM/20/235215

Abstract

A model for the transformation of an Al–Cu–Fe icosahedral quasicrystal into a crystal with a B2-type phase is proposed. The model is based on two assumptions: (1) the main building block for the quasicrystal structure is a hierarchical dodecahedron composed of two icosahedral clusters, coinciding with two different sections of the {3, 3, 5} polytope; (2) the transformation of the quasicrystal into a B2-type crystal phase can be described as the transition between 3D sections of two polytopes, namely {3, 3, 5} and {3, 4, 3}. In the framework of the proposed model, two experimental facts gain plausible explanations: the transformation of the Al–Cu–Fe quasicrystal into the BCC phase specifically and the orientational relationships observed between this BCC phase and the initial icosahedral quasicrystal.

1. Introduction

In most cases quasicrystals are transformed into so-called approximate crystalline phases having very large unit cells and electron diffraction patterns which are very similar to the diffraction patterns of quasicrystals. Some time ago, the experimental observation of the transformation of an Al₆₂Cu_{25.5}Fe_{12.5} icosahedral quasicrystal (IQC) into the crystalline BCC phase (disordered CsCl-type) was published [1]. The transformation was induced by surface scratching of a quasicrystal with a WC–Co cermet indenter. The close orientational relationships between the cubic phase and the Al–Cu–Fe IQC were determined as follows:

$$\langle 110 \rangle, \langle 113 \rangle \parallel A5$$

and

$$\langle 110 \rangle, \langle 111 \rangle, \langle 112 \rangle \parallel A2.$$

Later, a mechanism was proposed for the quasicrystal–crystal transformation [2]. This model mechanism was based on considering the eight-dimensional (8D) root lattice E_8 as the prophase (prototype phase) for any polymorphic transformation. On a local level, the transformation was described as a mutual reconstruction of the coordination polyhedra of transformation participants [2]. In such terms, the phase participating in the transformation and the intermediate configurations through which the transformation was effected could be treated as structural realizations of specific constructions of algebraic geometry. Experimental support for the proposed mechanism was found in the coincidence of the observed Miller indices for habit planes of iron martensite with Miller indices of the Frank–Kasper 14-vertex polyhedron. This polyhedron participates in the FCC–BCC transformation as an intermediate configuration. The reasons for the transformation of the IQC just into the BCC phase (disordered B2) are beyond the transformation model proposed in [2]. On the other hand, a model for the martensitic transformation of the BCC phase in titanium (and zirconium) has been proposed in [3], and this model is also based on the

⁴ Author to whom any correspondence should be addressed.

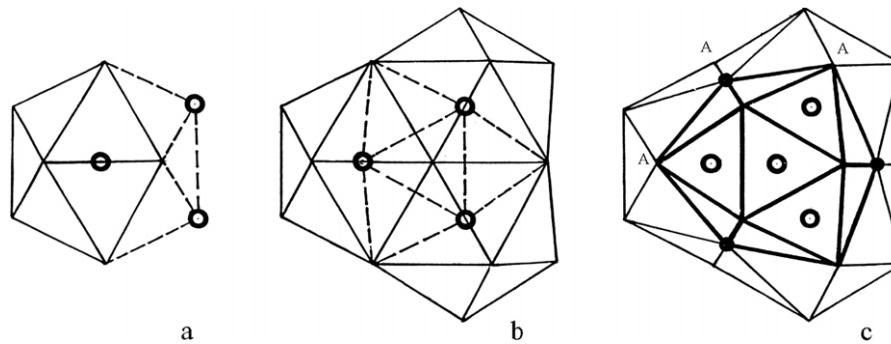


Figure 1. 3D sections of the $\{3, 3, 5\}$ polytope started from a polytope vertex (a), face (b) or a polytope cell (c). All sections exist as fragments of the crystalline lattice of certain intermetallics. The cluster with the D_{3h} symmetry (b) is the intersection of three icosahedra; it forms the structure of Al_3Co_2 , $Al_{10}Mn_3$, Al_9Mn_3Si and other compounds. Open circles denote positions of transition metal atoms, the remaining vertices are occupied by Al atoms. The cluster with the T_d -symmetry (c) is the intersection of four icosahedra; it forms the structure of Ti_2Ni , $Al_{13}Cr_4Si_4$, Fe_3W_3C , Cu_5Zn_8 (γ -brass), Th_6Mn_{23} and others. In the case of $Al_{13}Cr_4Si_4$ open circles denote positions of Cr atoms and dark circles the positions of Si atoms, and the remaining vertices are occupied by Al atoms. Vertices denoted by letters A form an octahedron.

eight-dimensional root lattice E_8 as the prototype phase. In the present work, we propose a model to explain why the IQC in the Al–Cu–Fe system transforms just into the crystalline phase with the BCC structure.

2. Model

Obviously, both the IQC \rightarrow BCC crystal transformation and the orientational relationships between an initial IQC and its crystalline transformation products are determined by: (1) the local quasicrystal structure and (2) the transformation mechanism. A widely accepted description of the quasicrystal phenomenon is the strip-projection method (SPM) on the basis of six-dimensional (6D) primitive (P), FCC and BCC lattices [4]. For example, the unit cell of a 6D primitive cubic lattice with its $2^6 = 64$ vertices is mapped onto a triacontahedron with 32 vertices in 3D Penrose tiling. All these lattices are so-called root lattices B_6 (P lattice), D_6 (FCC lattice) and D_6^* (BCC lattice) [5]. Here the asterisk denotes a dual lattice. A generalized SPM permits us to obtain a more complex tiling than 3D Penrose models for the quasicrystal structure. For example, icosahedral Danzer tiling can be derived from the D_6 lattice [6]. In that tiling different windows determine different classes for the meeting of polyhedra at the common vertex. Atomic decorations of the quasicrystal structure models in the frameworks of the SPM are mainly confined to the known Mackay cluster or Bergman cluster [7].

However, there is a more general and complete description of the quasicrystal structure. All 6D lattices are sublattices of the 8D root lattice E_8 so they can be inserted into it (see [8]). Due to this the symmetry of the root lattice E_8 includes all symmetries described by Yamamoto [4]. A detailed description of the connection of the quasicrystal structure with the E_8 lattice was presented by Sloane and Elser [9], Sadoc and Mosseri [10, 11] and Moody and Patera [12]. We will show here that an adequate model for the IQC with real atomic decorations can be constructed in the framework of the E_8 lattice concept only.

Earlier, a geometric model was proposed for the 3D space structure of icosahedral [13] and decagonal [14] quasicrystals.

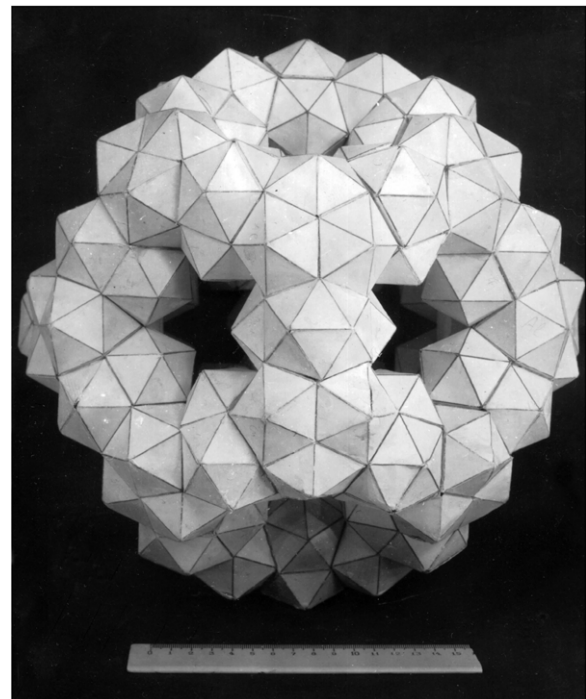


Figure 2. Photo of the cartoon model of a hierarchical dodecahedron formed by sticking together clusters from figure 1 in the $D_{3h}-T_d-D_{3h}-T_d-\dots$ sequence. The photo is taken along the two-fold axis of the dodecahedron.

In both cases the quasicrystal structures were constructed from two starting clusters with D_{3h} and T_d symmetries (figure 1), these clusters were taken from experimental data as fragments of crystal structures of certain intermetallics (see caption to figure 1). By sticking these two clusters through their common corrugated hexacycles in the $D_{3h}-T_d-D_{3h}-T_d-\dots$ sequence one can generate a hierarchical dodecahedron with an edge length of 0.7–0.75 nm (figure 2) which is considered in [13] as the main building block for the quasicrystal structure. That model gave a satisfactory explanation for the origin of the non-crystallographic icosahedral symmetry of the

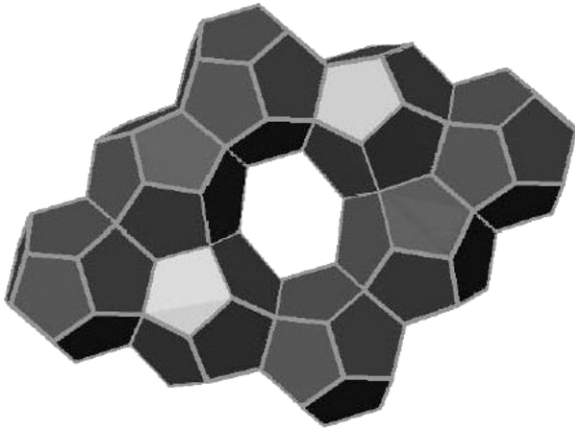


Figure 3. Rolling of the $\{5, 3, 3\}$ polytope along four rhombus edges generates a $-2\pi/5$ disclination threading the center of the rhombus face (see the six-membered ring in the center) [18].

point diffraction patterns, positions of diffraction maxima and chemical composition of quasicrystalline phases. However, analysis for the possible correspondence of the proposed model with SPM or with the E_8 concept used in [9–12] was not conducted in [13, 14].

D_{3h} and T_d clusters and the composite dodecahedron could be considered as the spherical shells which are determined by 3D projections of the $\{3, 3, 5\}$ polytope. A single icosahedron (figure 1(a)) is the part of the projection started from the polytope vertex. A cluster with D_{3h} symmetry is the projection started from a polytope face (figure 1(b)) while the third cluster with the T_d symmetry is the projection started from a tetrahedral cell (figure 1(c)). Distortions of tetrahedron edges are needed for this straightening of polytope substructures. Necessary distortions have been effected by positioning different atomic species in different vertices. Bearing in mind the description by Sadoc and Mosseri in [10] of the 8D lattice E_8 as a set of concentric icosahedral shells, the dodecahedron shown in figure 2 can be regarded as joining of icosahedral shells determined by the root lattice E_8 .

It can be noted that Mackay and Bergman clusters are also 3D projections from the $\{3, 3, 5\}$ polytope started from a vertex. In our model we use polytope projections started from a face and a cell for the first time.

The possibility for sticking these D_{3h} and T_d clusters is determined by their derivation as polytope sections. Since both clusters consist of joined $\{3, 3, 5\}$ polytope sections, in the interior of this polytope they could be joined without intersection along the common three-fold axis (that is the 6_1 axis in the polytope). In other words, a linear substructure is delineated in the $\{3, 3, 5\}$ polytope, and this substructure can be represented as the sequence of three clusters T_d – D_{3h} – T_d . As has been said above, the $\{3, 3, 5\}$ polytope is determined by the E_8 lattice, and the E_8 lattice also determines a dual $\{5, 3, 3\}$ polytope, and the $\{720\}$ polytope as they join [9]. In the latter the edge of the dodecahedral cell of the $\{5, 3, 3\}$ polytope is perpendicular to a triangular face of the $\{3, 3, 5\}$ polytope and runs through the face center. Each one of the 600 cells of the $\{3, 3, 5\}$ polytope is centered by a vertex belonging to the

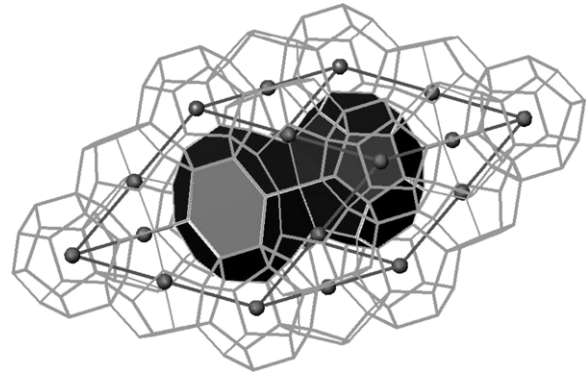


Figure 4. A rhombohedron decorated by dodecahedra with two hexakaidecahedra inside. The rhombohedron serves as one branch of a 20-branched dodecahedral star. Centers of hexakaidecahedra are intersecting points of four disclination segments.

dual $\{5, 3, 3\}$ polytope; respective joining of the $\{3, 3, 5\}$ and $\{5, 3, 3\}$ polytopes gives 720 vertices which can be regarded as the 4D counterpart of the triacontahedron [9]. In such a way the axis of the selected linear substructure (i.e. the T_d – D_{3h} – T_d sequence) coincides with the edge of the dodecahedron from $\{5, 3, 3\}$, which is also a part of the $\{720\}$ polytope. All vertices of the selected linear substructure of $\{3, 3, 5\}$ correspond to D_{3h} symmetry, so we can state that this substructure can be inserted into the decorated $\{5, 3, 3\}$ polytope ($\{5, 3, 3\}_{dec}$). As a result, the dodecahedral cluster shown in figure 2 can also be inserted into the decorated $\{5, 3, 3\}_{dec}$ polytope corresponding to the set of icosahedral shells in the root lattice [10], and it must be regarded as the decorated cell of $\{5, 3, 3\}_{dec}$. Both edge length and diameter of the decorated polytope are determined by experiment, since we are joining together only clusters which have been observed experimentally.

The next step of the quasicrystal model construction is filling of the 3D space by hierarchical dodecahedra. Since the tessellation of the 3D Euclidean space onto regular dodecahedra is impossible, one must use the scheme of polytope straightening including rolling the polytope over the 3D hyperplane and introducing defects (disclinations) [15–17]. Ishii [18] has considered the rolling of the $\{5, 3, 3\}$ polytope along its 10_1 symmetry axis. While rolling along a single direction the rod-like substructure is generated, containing dodecahedra joined in the face-to-face mode. While rolling the dodecahedral cell along four rhombus edges the defect arises in the center of the rhombus face.

That defect is the $-2\pi/5$ disclination threading a six-membered ring in the face center (see figure 3). Six rhombus faces formed by rolling dodecahedral cells are joined into a prolate rhombohedron (figure 4), and disclinations threading face centers intersect at two points belonging to the space diagonal of the rhombohedron. Disclination segments are intersecting under tetrahedral angles. As a result, a hole inside the rhombohedron has the shape of two hexakaidecahedra connected by the inversion center in a common hexagonal face. Since dodecahedra can be joined into both prolate and oblate rhombohedra (see [19]), in the next step one can obtain the 3D Penrose tessellation

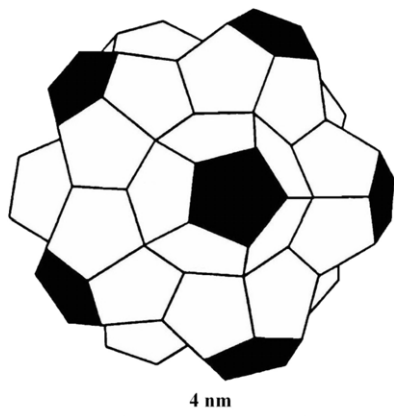


Figure 5. Joining of the hierarchical dodecahedra shown in figure 2 by the face-to-face mode starts the assemblage of the dodecahedral star (20-branched stellated polyhedron).

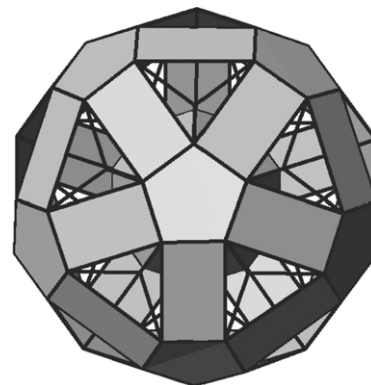


Figure 7. Two shells of the disclination network. The outer shell is a rhombicosidodecahedron and the inner shell is the dodecahedron. Shells are connected by radial segments along three-fold axes.

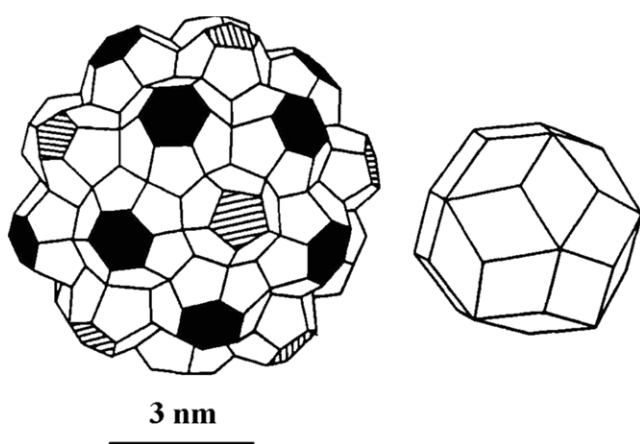


Figure 6. The next step in the assemblage of the 20-branched stellated polyhedron (dodecahedral star). The centers of hexakaidecahedra (with black hexagonal faces) form a dodecahedron (an inner shell of the disclination network). Centers of hexakaidecahedra and dodecahedra taken together form a rhombic triacontahedron (right).

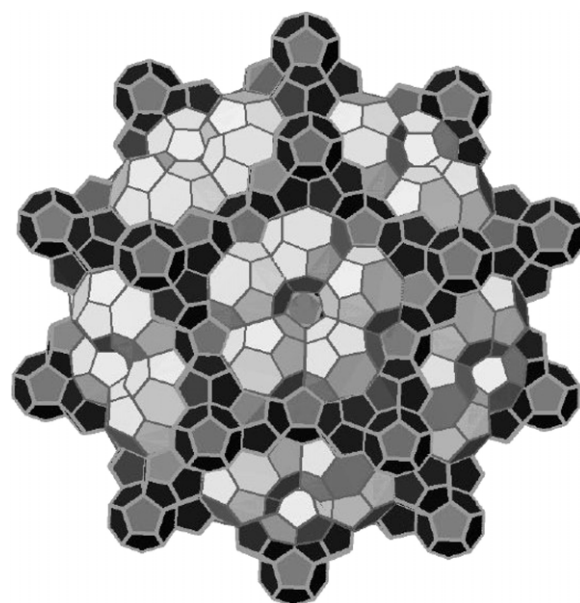


Figure 8. The limiting cluster with icosahedral symmetry is a hierarchical dodecahedral star. The outer cluster shell overlaps with neighboring clusters having the same structure. This hypercluster with a diameter of about 16 nm serves as the cooperative atom in the quasicrystal structure.

with rhombohedra decorated by the hierarchical dodecahedra shown in figure 2. This step corresponds to Mackay’s proposal for decoration of the 3D Penrose tessellation by dodecahedral cells [20]. Our approach is distinguished by the use of a hierarchical dodecahedron instead of an ordinary polyhedron. While sticking dodecahedra into a rhombohedron unavoidable gaps arise between them [19]. In the case of the hierarchical dodecahedron gaps can be eliminated easily by edge deformation, since the edge is not a single interatomic bond but is formed by several tens of bonds.

In accordance with accepted quasicrystal models based on the SPM and 6D lattice the icosahedral symmetry of their point diffraction patterns is ensured by the presence of the 20-branched star-polyhedron (the dodecahedral star) in the 3D Penrose tessellation. This dodecahedral star is formed by joining of 20 prolate rhombohedra in one common vertex [7]. The sequential steps of constructing such a polyhedron from hierarchical dodecahedra are depicted in figures 4–8. Details of the atomic structure of hierarchical

polyhedra are not shown on these pictures; for clarity they are represented as ordinary polyhedra with straight edges. The disclination network is generated while joining 20 hierarchical rhombohedra (see figure 7). That disclination network consists of two concentric shells: the knots of the inner shell (centers of the hexakaidecahedra) form a dodecahedron (see figure 6), while the knots of the outer shell form a rhombicosidodecahedron. Shells are connected with each other by the radial disclination segments oriented along three-fold symmetry axes of the dodecahedral star. The result of the star assembly is shown in figure 8. The hierarchical cluster with icosahedral symmetry represents the joining of the polytope sections determined by the root lattice E_8 [9, 10]. As can be seen, the centers of the hexakaidecahedra (i.e. knots of the disclination network) form the rhombicosidodecahedron

(an outer shell of the disclination network in figure 7). It is the maximal possible cluster since after adding the next polyhedral shell (dodecahedra and hexakaidecahedra) 12 similar clusters form around five-fold axes.

Pentagonal faces of the rhombicosidodecahedron are shared between two neighboring hierarchical clusters, so these new clusters are interpenetrating with the central cluster along five-fold axes and oriented parallel to each other. The limiting cluster contains 195 dodecahedra and 100 hexakaidecahedra (40 in the interior of 20 rhombohedra and 60 in the vertices of the rhombicosidodecahedron).

The final hierarchical cluster has a diameter of about 16 nm. It can serve as ‘a cooperative atom’ for both aperiodic and periodic models, i.e. for the IQC and its crystalline approximant. Since it contains approximately 1.5×10^5 ordinary (‘chemical’) atoms and has an icosahedral symmetry, in the ordinary diffraction experiment one cannot distinguish between aperiodic and periodic stacking of such giant ‘quasi-atoms’ oriented parallel to each other. Diffraction of electrons by parallel giant icosahedral clusters will give a point pattern corresponding to the cluster symmetry while the lattice period of the crystal formed by giant atoms is equal to about 32 nm [13]. Due to this, the assembled giant hierarchical cluster is simply pointing to the other possibility for explaining point diffraction patterns with icosahedral symmetry. Taking this explanation as valid there is no need to use concepts from the 3D Penrose tessellation and its crystalline approximant.

Taking this model of the icosahedral quasicrystal as the projection of the decorated $\{5, 3, 3\}_{dec}$ polytope, both the transformation of the IQC into the disordered B2-phase and the orientation relationship between them observed in [1] can be easily explained.

Edges of the hierarchical dodecahedron (figure 2) are decorated by clusters with the D_{3h} symmetry representing joining of three icosahedra and coinciding, as was said above, with the 3D projection of the $\{3, 3, 5\}$ polytope starting from a face (vertices of this face are shown on figure 1(b) by open circles). The common part of three icosahedra (delineated as a dotted line in figure 1(b)) contains 11 vertices belonging to 11 tetrahedra. As was shown in [3], this 11-vertex cluster serves as intermediate configuration during the martensitic BCC–HCP transformation.

The essence of the model proposed in [3] for the BCC–HCP transformation is depicted in figure 9. Here two 11-vertex clusters are shown where the first cluster is the joining of three distorted octahedra about a common edge C–C (figure 9(a)). That octahedral cluster is the fragment of the hexagonal crystalline lattice of the ω -phase which is the intermediate product of the martensitic transformation in titanium- and zirconium-based alloys [21]. The common edge of three octahedra is parallel to the $[0001]_{\omega}$ direction of the ω structure. Joining three octahedra around a common edge determines the $\{3, 4, 3\}$ polytope having 24 vertices and 24 octahedral cells in 4D space [22], so the 11-atom fragment of the ω structure shown in figure 9(a) coincides with the section of $\{3, 4, 3\}$ by a 3D hyperplane drawn from an edge.

Skipping the common C–C edge in the 11-atom octahedral cluster of the ω phase and inserting three new bonds between

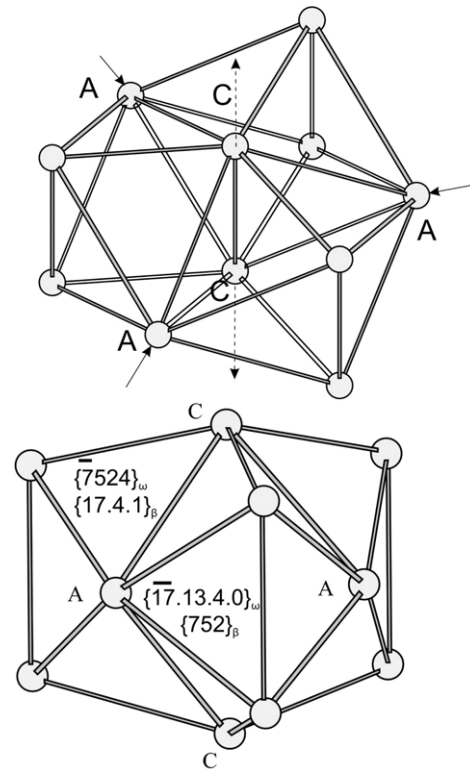


Figure 9. Reconstruction of the 11-atom octahedral cluster (top) into the 11-atom tetrahedral cluster (bottom) by elongating the C–C edge and compressing the cluster in the A–A–A plane (see arrows). The 11th atom A in the tetrahedral cluster is invisible. Miller indices of different faces are shown in the hexagonal and cubic settings. All outer edges of the cluster are equal to each other, whereas inner edges A–A are elongated by 18%.

the A vertices lying in the horizontal mirror plane of the cluster generates a new 11-atom cluster representing in itself the joining of 11 tetrahedra in the face-to-face mode, i.e. the section of the $\{3, 3, 5\}$ polytope started from a face (figure 9(b)). In the $\{3, 3, 5\}$ polytope each vertex serves as the center of an icosahedron, therefore each atom in the 11-atom tetrahedral cluster can be surrounded by 12 atoms occupying icosahedral vertices. This 11-atom tetrahedral cluster is the product of a mutual intersection of three icosahedra, whereas each vertex of the central triangle in the $(0001)_{\omega}$ plane serves as an icosahedron center. Thus, as a result of a deformation of the 11-atom octahedral cluster of the ω phase we obtain the 11-atom tetrahedral cluster and vice versa. We can say that BCC–HCP transformation is the transition from the straightened fragment of the $\{3, 4, 3\}$ polytope to the straightened fragment of the $\{3, 3, 5\}$ polytope. The said transition from one polytope into the other was achieved by deformation only; the number of vertices is unchanged. Of course, there is a fundamental connection between both polytopes: according to the Gosset scheme [23], an action of the five-fold symmetry axis on 24 vertices of the $\{3, 4, 3\}$ polytope generates 120 vertices of the $\{3, 3, 5\}$ polytope.

We can obtain hexagonal packing directly from the BCC packing, since it is known that an icosahedron can be reconstructed into an anti-cuboctahedron with HCP

polytope from the 6D D_6 lattice, but the $\{3, 3, 5\}$ polytope, dual to it the $\{5, 3, 3\}$ polytope, their joining $\{720\}$ polytope, and the D_6 lattice can be obtained from the E_8 lattice.

The existence of the Mackay cluster in the real crystal structure of the cubic α -AlMnSi phase [33] serves as experimental support for the quasicrystal models decorated by these clusters. However, there is also the β -AlMnSi phase having hexagonal structure and the same chemical composition as the α -AlMnSi phase [34]. This β -AlMnSi is isomorphic with the Al_5Co_2 phase, i.e. its structure is composed from the same icosahedral triplets, as was shown above in figure 1(b). Le Lann [35] did show the equivalence between the descriptions of icosahedral quasicrystals in the framework of the SPM by ' α -AlMnSi-like' and ' β -AlMnSi-like' decorations of the 6D cubic lattice. Moreover, the icosahedral $Al_{73}Mn_{21}Si_6$ alloy transforms entirely into the β -AlMnSi phase by heating at 700 °C [36].

Also, a metric correspondence can be found between our model and the 6D description of the quasicrystal structure. The length of the icosahedron diagonal in the T_d and D_{3h} clusters (figure 1) is equal to $\tau d_{Al} = 0.46$ nm, since the icosahedron edge length is equal to the atomic diameter of aluminum, $d_{Al} = 0.286$ nm, and the golden number $\tau = 1.618$. But the value of 0.46 nm is exactly the so-called quasilattice period a_R in the 6D formalism [37]. Also, the period of the periodical packing of the hierarchical giant clusters $a_{qc} = 50\tau^3(\tau + 2)^{-1/2}d_{Al} = 50d_5$ [13], where d_5 is the diameter of a sphere inscribed into a dodecahedron with aluminum atoms in its vertices. The d_5 value of 0.637 nm is very close to the edge length of the 6D-cube determined from the diffraction data [37].

Chemical composition of the hierarchical dodecahedron in figure 2 is in close coincidence with the experimentally observed chemical composition of the IQC. As was shown in [14], if the central triangle of the D_{3h} cluster (open circles in figure 1(b)) and the centers of its hexacycles, the central tetrahedron and the centers of the hexacycles of the T_d cluster in figure 1(c) are occupied by manganese atoms, and all the other vertices with aluminum atoms, then the chemical composition of the IQC is described by the formula $Al_{17}Mn_5$ ($Al_{77.3}Mn_{22.7}$). If the central triangle of the D_{3h} cluster and the central tetrahedron of the T_d cluster are occupied by Cu atoms and the type-A vertices (forming a large octahedron) by Fe atoms whereas all the other vertices are occupied by aluminum atoms, then the composition of the IQC will be $Al_{14}Cu_5Fe_3$, i.e. $Al_{63.6}Cu_{22.7}Fe_{13.6}$. Both predicted compositions are close to the experimentally observed IQC compositions in Al–Mn and Al–Cu–Fe alloy systems, respectively.

Bearing in mind the idea put forward by Mackay [30] we have used a similar model of the hierarchical cluster to explaining the phenomenon of so-called aperiodic phases with the cubic symmetry [38]. Such objects observed in the melt quenched Mg–Al alloys have been designated as 'quasicrystals without forbidden symmetry axis' [39]. In the framework of our approach the appearance of aperiodic diffraction patterns can be explained in a unique way independently of their non-crystallographic or crystallographic symmetry. Both the IQC and cubic aperiodic phases are objects with the hierarchical principle of structural organization of condensed matter.

As a final remark, we want to point out that the outer morphology of the growing IQC is in some cases a dodecahedral one and in some cases a triacontahedral morphology or dodecahedral star [40], but in no cases were icosahedral quasicrystals growing with icosahedral morphology.

4. Conclusion

- (1) An atomic model of the icosahedral phase can be constructed as the hierarchical joining of 3D sections of the 4D polytopes determined by the 8D root lattice E_8 .
- (2) The hierarchical construction has been obtained by decoration of the $\{720\}$ polytope, determined by the E_8 lattice and representing the joining of the $\{3, 3, 5\}$ and $\{5, 3, 3\}$ polytopes. The cell of the $\{5, 3, 3\}$ polytope was decorated by vertices of two different 3D sections of the $\{3, 3, 5\}$ polytope. Both sections used for the decoration have been experimentally observed as clusters belonging to the crystal structures of certain intermetallic compounds, so the edge length and diameter of the decorated polytope is determined by experiment.
- (3) The decorated $\{5, 3, 3\}$ polytope can be mapped onto three-dimensional Euclidean space by the known route of rolling its hierarchical dodecahedral cell along edges of the rhombohedron. The obtained hierarchical rhombohedron can have aperiodic Penrose tiling or periodic crystallographic tiling. Since the lattice period of the crystallographic tiling is about 32 nm, a distinction between aperiodic and periodic (approximant) tiling is not possible in the standard diffraction experiment.
- (4) In the framework of this model it is possible to explain accurately two experimental facts: the transformation of the Al–Cu–Fe quasicrystal into the BCC phase specifically and the orientational relationships between this BCC phase and an initial icosahedral quasicrystal.
- (5) The transformation of an icosahedral quasicrystal into the cubic B2 phase can be considered as the transition from a 3D section of the $\{3, 3, 5\}$ polytope into the 3D section of the $\{3, 4, 3\}$ polytope. This description is quite similar to the recently suggested description for the BCC–HCP transformation.

Acknowledgments

This work was supported by a grant of the Chemical Department of RAS, program no. 7, grants of the Presidium RAS 'Innovation sponsoring-2007', 'Innovation sponsoring-2008', Russian Foundation for Basic Research (RFBR) grant no. 08-02-01177-a.

References

- [1] Wu J S, Brien V, Brunet P, Dong C and Dubois J-M 2000 Electron microscopy study of scratch-induced surface microstructures in an Al–Cu–Fe icosahedral quasicrystal *Phil. Mag. A* **80** 1645–55

- [2] Kraposhin V S, Talis A L and Dubois J-M 2002 Structural realization of the polytope approach for the geometrical description of the transition of a quasicrystal into a crystalline phase *J. Phys.: Condens. Matter* **14** 8987–96
- [3] Kraposhin V S, Talis A L and Wang Y J 2006 Description of polymorphic transformations of Ti and Zr in the framework of the algebraic geometry *Mater. Sci. Eng. A* **438–440** 85–9
- [4] Yamamoto A 1996 Crystallography of quasiperiodic crystals *Acta Crystallogr. A* **52** 509–60
- [5] Conway J H and Sloane N J A 1988 *Sphere-Packings, Lattices and Groups* (Berlin: Springer)
- [6] Danzer L, Papadopolos Z and Talis A 1993 Full equivalence between Socolar's tiling and the (A, B, C, K)-tillings leading to a rather natural decoration, *Int. J. Mod. Phys. B* **7** 1379–86
- [7] Janot C 1994 *Quasicrystals* 2nd edn (New York: Cambridge University Press)
- [8] Humphreys J E 1975 *Linear Algebraic Groups* (New York: Springer) section 35
- [9] Elser V and Sloane N J A 1987 A highly symmetric four dimensional quasicrystal *J. Phys. A: Math. Gen.* **20** 6161–8
- [10] Sadoc J F and Mosseri R 1993 The E₈ lattice and quasicrystals: geometry, number theory and quasicrystals *J. Phys. A: Math. Gen.* **26** 1789–809
- [11] Sadoc J F and Mosseri R 1993 The E₈ lattice and quasicrystals *J. Non-Cryst. Solids* **153/154** 247–52
- [12] Moody R V and Patera J 1993 Quasicrystals and icosians *J. Phys. A: Math. Gen.* **26** 2829–53
- [13] Kraposhin V S 1996 Assembly of an icosahedral quasicrystal from hierarchic atomic clusters *Crystallogr. Rep.* **41** 371–80
- [14] Kraposhin V S 1999 Assembly of an icosahedral quasicrystal from hierarchic atomic clusters: decagonal symmetry *Crystallogr. Rep.* **44** 927–37
- [15] Nelson D R 1983 Order, frustration, and defects in liquids and glasses *Phys. Rev. B* **28** 5515–35
- [16] Mosseri R and Sadoc J F 1984 Hierarchical structure of defects in non-crystalline sphere packings *J. Phys. Lett.* **45** L827–32
- [17] Mosseri R and Sadoc J F 1986 Polytopes and projection method: an approach to complex structures *J. Phys. Coll.* **47** (Suppl.) C3 281–97
- [18] Ishii I 1988 Propagating local positional order in tetrahedrally bonded systems *Acta Crystallogr. A* **44** 987–98
- [19] Lord E A, Mackay A L and Ranganathan S 2006 *New Geometries for New Materials* (New York: Cambridge University Press)
- [20] Mackay A L 1985 Icosahedra in aluminium/manganese alloy *Nature* **315** 636
- [21] McQuillan M K 1963 Phase transformations in titanium and its alloys *Metall. Rev.* **8** N29
- [22] Coxeter H S M 1983 *Regular Polytopes* (New York: Dover)
- [23] Mosseri R, DiVincenzo D P, Sadoc J F and Brodsky M H 1985 Polytope model and the electronic and structural properties of amorphous semiconductors *Phys. Rev. B* **32** 3974–4000
- [24] Shalaeva E V and Prekul A F 2000 Structure state of β -solid solution in quenched quasicrystal-forming alloys of Al₆₁Cu₂₆Fe₁₃ *Phys. Status Solidi a* **180** 411–25
- [25] Faydot F, Quivy A, Calvayrac Y, Gratias D and Harmelin M 1991 *Mater. Sci. Eng. A* **133** 383–7
- [26] Yokoyama Y, Fukaura K, Sunada H, Note R, Hiraga K and Inoue A 2000 *Mater. Sci. Eng. A* **294–296** 68–73
- [27] Lidin S 1991 Quasicrystals: local structure versus global structure *Mater. Sci. Eng. A* **134** 893–5
- [28] Janot C M and de Boissieu M 1994 Quasicrystals as a hierarchy of clusters *Phys. Rev. Lett.* **72** 1674–7
- [29] Ebert P, Feuerbacher M, Tamura N, Wollgarten M and Urban K 1996 Evidence for a cluster-based structure of AlPdMn single quasicrystals *Phys. Rev. Lett.* **77** 3827–30
- [30] Mackay A 1998 Some are less equal than others *Nature* **391** 334–5
- [31] Tsai A P, Guo J Q, Abe E, Takakura H and Sato T J 2000 A stable binary quasicrystal *Nature* **408** 537–8
- [32] Le Lann A 1992 Three-dimensional F quasilattice model of decoration for Al–Cu–Fe icosahedral alloys *Phil. Mag. B* **66** 653–65
- [33] Cooper M and Robinson K 1966 The crystal structure of the ternary alloy α (AlMnSi) *Acta Crystallogr.* **20** 614–7
- [34] Robinson K 1952 The structure of β (AlMnSi)–Mn₃SiAl₉ *Acta Crystallogr.* **5** 397–403
- [35] Le Lann A 1990 Structure of the icosahedral Al–Mn–Si alloys: decoration in three-dimensional space of a six-dimensional cubic I lattice *Phil. Mag. B* **62** 577–87
- [36] Calvayrac Y, Devaud-Rzepski J, Bessière M, Lefebvre S, Quivy A and Gratias D 1989 The nature of the topological disorder in the rapidly quenched Al₇₃Mn₂₁Si₆ icosahedral phase *Phil. Mag. B* **59** 439–50
- [37] Ranganathan S and Chattopadhyay K 1991 Quasicrystals *Annu. Rev. Mater. Sci.* **21** 437–62
- [38] Kraposhin V S, Talis A L and Ha Thanh L 2008 The structure model of a cubic aperiodic phase ('quasicrystal without forbidden symmetry axes') *J. Phys.: Condens. Matter* **20** 114115
- [39] Donnadieu P, Harmelin M, Su H-L, Seifert H-J, Effenberg G and Aldinger F A 1997 Quasicrystal with inflation symmetry and no forbidden symmetry axes in a rapidly solidified Mg–Al alloy *Z. Metallk.* **88** 33–7
- [40] Abe E, Yan Y and Pennycook S J 2004 Quasicrystals as cluster aggregates *Nat. Mater.* **3** 759–67